

Microbial pterins as potential indicators of organic carbon dynamics in estuarine and coastal sediments

Kang Mei^{a,b,g,*}, Yitong Pan^c, Danny Alejandro Osorio^d, Lizhe Cai^e, Hualong Hong^e, Mohammad Mazbah Uddin^f, Song Wang^a, Xin Xiao^a, Xuri Dong^a, Li Chen^{a,g}, Shicong Xiao^{a,b}, Deli Wang^{b,g,**}

^a Jiangsu Institute of Marine Resources Development, Jiangsu Key Laboratory of Marine Bioresources and Environment, Jiangsu Ocean University, Lianyungang 222005, China

^b State Key Laboratory of Marine Environmental Science, College of Ocean and Earth Sciences, Xiamen University, Xiamen 361102, China

^c Department of Civil and Environmental Engineering, Princeton University, Princeton, NJ 08544, USA

^d Department of Biological Sciences, University of Southern California, Los Angeles 90089 CA, USA

^e Key Laboratory of Ministry of Education for Coastal and Wetland Ecosystems, College of the Environment and Ecology, Xiamen University, Xiamen 361102, China

^f Key Laboratory of the Ministry of Education for Earth Surface Processes & College of Urban and Environmental Sciences, Peking University, Beijing 100089, China

^g Jiangsu Marine Resources Development Technology Innovation Center, Lianyungang 222042, China

ARTICLE INFO

Keywords:

Microbial Pterins
Trace biomarker molecules
Chlorophyll-a
Sediment organic carbon
Estuarine wetlands
Ecological indicator

ABSTRACT

Pterins serve as precursors, pigments, and enzymatic cofactors in microbes, contributing to global nutrient cycles and unconventional carbon and nitrogen utilization. This study investigated the biogeochemical characteristics of microbial pterins in the Jiulong River Estuary and Xiamen Bay, focusing on their spatiotemporal distribution in estuarine wetlands during dry and flood seasons. However, the ecological significance of pterins as biomarkers for carbon accumulation and degradability in estuarine sediments remains underexplored, limiting their application in monitoring coastal carbon sinks and algal bloom dynamics. By analyzing correlations between environmental factors and biological indices, we provide novel insights into estuarine ecological processes. Our results indicate that during the flood season, phytoplankton, including freshwater algae and cyanobacteria, are the primary sources of microbial pterins, driven by high productivity from upstream inputs. In the dry season and under reducing sediment conditions, heterotrophic contributions to microbial pterins become more prominent. Dihydro-neopterin and neopterin dominate in reducing sediments, while biopterin and its metabolite iso-xanthopterin are more prevalent in the water column. The strong correlation between chlorophyll *a* and pterins suggests that microbial pterins co-vary with phytoplankton biomass and may serve as indicators of marine algal blooms. Increased pterin levels signal bloom initiation, while their rapid consumption marks bloom progression. Additionally, sediment C/N ratio and iso-xanthopterin levels hint at the potential use of pterins as biomarkers for revealing coastal carbon dynamics. These findings highlight the need for further research on the role of pterins in carbon cycling and their application in monitoring marine ecosystems.

1. Introduction

Pterins are essential biomolecules in microorganisms, functioning as enzymatic cofactors in diverse metabolic pathways, including UV protection, intracellular signaling, and nutrient metabolism (Feirer and Fuqua, 2017). Their roles extend to photosensitized singlet oxygen reactions and the metabolism of amino acids and nucleotides (Arpa and

Corral, 2023; Buglak et al., 2022), while their structural backbone is integral to the biosynthesis of folate (B_9) and riboflavin (B_2)—vitamins critical for microbial growth and redox balance (Basu and Burgmayer, 2011b; Gorelova et al., 2019). Bacterial pterins were first identified in cyanobacteria (Feirer and Fuqua, 2017), such as *Anacystis*, *Anabaena*, and *Nostoc* (Forrest et al., 1957; Forrest et al., 1958), pterins like tetrahydrobiopterin (BH_4) regulate aromatic amino acid hydroxylation and

* Corresponding author at: Jiangsu Institute of Marine Resources Development, Jiangsu Key Laboratory of Marine Bioresources and Environment, Jiangsu Ocean University, Lianyungang 222005, China.

** Corresponding author.

E-mail addresses: kangmei@jou.edu.cn (K. Mei), deliwang@xmu.edu.cn (D. Wang).

nitrogen assimilation, enabling microbes to adapt to fluctuating carbon and nitrogen sources (Daubner and Fitzpatrick, 2013; Feirer and Fuqua, 2017). Cyanobacteria further utilize pterin glycosides for light harvesting and nitrogen fixation (Chung et al., 2000; Zuo et al., 2022), with biopterin derivatives acting as UV-A absorbing pigments that enhance photosynthetic efficiency (Matsunaga et al., 1993; Wachi et al., 1995). Despite their ecological significance, the biogeochemical roles of microbial pterins in marine systems remain underexplored, particularly in estuarine sediments—dynamic interfaces where organic carbon (OC) accumulation and degradation shape coastal carbon sinks.

Estuarine wetlands are critical zones for sediment organic carbon (SOC) sequestration, driven by tidal inputs, phytoplankton carbon fixation, and terrestrial organic matter deposition (Cai et al., 2021; Mao et al., 2022; Xie et al., 2023). These ecosystems exhibit SOC accumulation rates up to tenfold higher than inland wetlands (Lu et al., 2017; Xie et al., 2023), yet rapid urbanization and nutrient enrichment in China have disrupted estuarine biogeochemical cycles, fostering eutrophication and recurrent algal blooms (Wang and Wang, 2016). Organic carbon in estuaries is partitioned between burial in sediments, export to the ocean, and release as dissolved organic carbon (DOC), with processes such as complexation, adsorption-desorption, and co-precipitation modulating SOC stability (Batchelli et al., 2010; Bruland and Lohan, 2004). However, the mechanisms governing SOC variability—particularly the interplay between microbial activity and environmental factors—remain poorly resolved, limiting predictive models of coastal carbon dynamics.

This study addresses these gaps by investigating microbial pterins as novel biomarkers for SOC cycling in the Jiulong River Estuary (JRE), a subtropical estuary in Southeast China. We focus on four key pterins: biopterin (BP), neopterin (NP), dihydro-neopterin (DNP), and iso-xanthopterin (IP)—metabolites derived from guanosine triphosphate (GTP) in photosynthetic and heterotrophic microbes. By analyzing their spatiotemporal distribution across dry and flood seasons, we aim to (1) elucidate hydrological and redox controls on pterin production, (2) evaluate correlations between pterins, chlorophyll-a (Chl-a), and sediment geochemistry, and (3) assess their potential as indicators of organic carbon accumulation and degradability. This work represents the first systematic field study linking microbial pterins to estuarine carbon dynamics, offering a framework to advance monitoring strategies for coastal carbon sinks and algal bloom management in rapidly changing environments.

2. Materials and methods

2.1. Study area

The study area is situated in Jiulong River Estuary (JRE) in Southeast China ($24^{\circ}24' - 24^{\circ}36'N$, $117^{\circ}40' - 118^{\circ}16'E$, Fig. S1). The JRE basin encompassed a basin area of approximately $15,000 \text{ km}^2$ (Wang et al., 2017), with an average water depth ranging from 3 to 18 m (Yu et al., 2019). Characterized as a semi-enclosed coastal region, the JRE experiences regular semi-diurnal tides and a subtropical monsoon climate, featuring wet seasons in spring and summer, and dry seasons in autumn and winter (Han, 2019; Pan et al., 2021). In this study, the flood period extended from May to September, while the dry period lasted from October to April (Fig. S1). The JRE discharges into the coastal waters of Xiamen Bay (XMB), situated at the southwestern entrance of the Taiwan Strait and bordered by the South China Sea and the Southwest Pacific Ocean to the east (Chen et al., 2021; Guo, 2005). The specific sampling stations selected in this study were divided into regions corresponding to the JRE (A3–A10, JY1–JY3) and the XMB (X1–X13).

2.2. Sampling and preparation

Surface and bottom water samples were collected using GO-FLO collectors at each site (General Oceanics, USA). The samples were

stored in high-density polyethylene (HDPE) bottles and pre-filtered on board using a 10- μm nylon sieve to remove impurities and large particles. Subsequently, a polycarbonate membrane (47 mm, 0.2 μm) filtration was employed at a low pumping pressure (<150 mm Hg) to separate particulate samples (0.2–10 μm) from 1 L pre-filtered seawater sample for microbial composition analysis. Particulate samples from 0.5 L pre-filtered seawater were collected similarly under clean conditions to determine microbial pterins concentrations.

Surface sediments were collected during four consecutive cruises along the same route in autumn (November 2020), winter (January 2021), spring (April 2021), and summer (July 2021). Sampling locations were determined based on on-site conditions as depicted in Fig. S1. Sediments were collected using a stainless grab-type sampler, and the top 5 cm of surface sediment was scraped and placed into 50 mL polypropylene centrifuge tubes for further processing. The sediment was homogenized before porewater extraction and soil-phase constituent analysis. Sediment and porewater were separated at 4000 rpm for 30 min using a low-speed centrifugation method (Bufflap and Allen, 1995; Lei et al., 2023). All samples were stored at -20°C in darkness before analysis.

2.3. Sediment and porewater geochemistry

The grain size for the freeze-dried sediment particle composition (Labconco Freeze Dryer 6.0 L, USA) was analyzed using a laser particle size analyzer (Mastersizer 3000, Malvern, UK). Sediment samples were treated with 20 % H_2O_2 to remove organic matter and 1 mol L^{-1} HCl to remove carbonate before measurement. Then, we removed the supernatant and added about 20 ml of 5 % sodium hexametaphosphate to the sample (Lu et al., 2023). The contents of total organic carbon (TOC) and total organic nitrogen (TON) in the sediments were measured by an elemental analyzer (Vario EL cube, Germany) after the samples were freeze-dried, ground, and sieved through 80 μm mesh net. Total organic matter (TOM) was quantified by the mass difference method after combusting the samples at 460°C for 6 h in a muffle furnace (Mei et al., 2023). Sediment pH and salinity were measured using a WTW multi-parameter meter (Multi 3430, Germany) after mixing the sediment with water at a soil-to-water ratio of 1: 2.5 and centrifuging to obtain the supernatant (Mei et al., 2020).

2.4. Chlorophyll-a and pterins determination

2.4.1. Chlorophyll-a measurement in solid and liquid phase

The content of Chl-a was extracted by adding 5 mL of 90 % acetone (v/v) to 1 g of fresh sediment and 3 mL of 90 % acetone (v/v) to 1 mL of pore water. The mixtures were incubated at -20°C in the dark for 24 h and then centrifuged at room temperature. The chl-a in the supernatant was detected using a fluorescence detector (Turner Designs Fluorometer, USA) (Liu et al., 2017). Pure Chl-a (Sigma Chemical) was used for calibration, and 90 % acetone was used as a blank control to exclude background fluorescence influence. The content of total Chl-a (T_Chla) in both solid and liquid phases was calculated as the sum of sediment Chl-a (S_Chla) and porewater Chl-a (P_Chla).

2.4.2. Microbial pterins extraction and quantification

Microbial pterins from sediment samples (1 g) and porewater samples (1 mL) were extracted following a previous study (Suffridge et al., 2017). All samples were mixed with 4 mL of cold lysis solution (5 % methanol: 95 % MQ water, v/v, adjusted to pH 3.5 with HCl) and 2 mL of zirconia/silica beads (5 mm, BioSpec, USA) in aseptic 15 mL polypropylene centrifuge tubes. Cells were lysed by vortexing with the beads for 5 min followed by ice bathing for 1 min, repeated six times over 30 min. Complete cellular lysis was confirmed by epifluorescence microscopy (Zeiss, Germany). The analyte pterins were incubated and extracted by ultrasonic bathing for 30 min in darkness at 30°C . The sample pH level was adjusted to 6.5 with 0.1 M NaOH. Pure chloroform

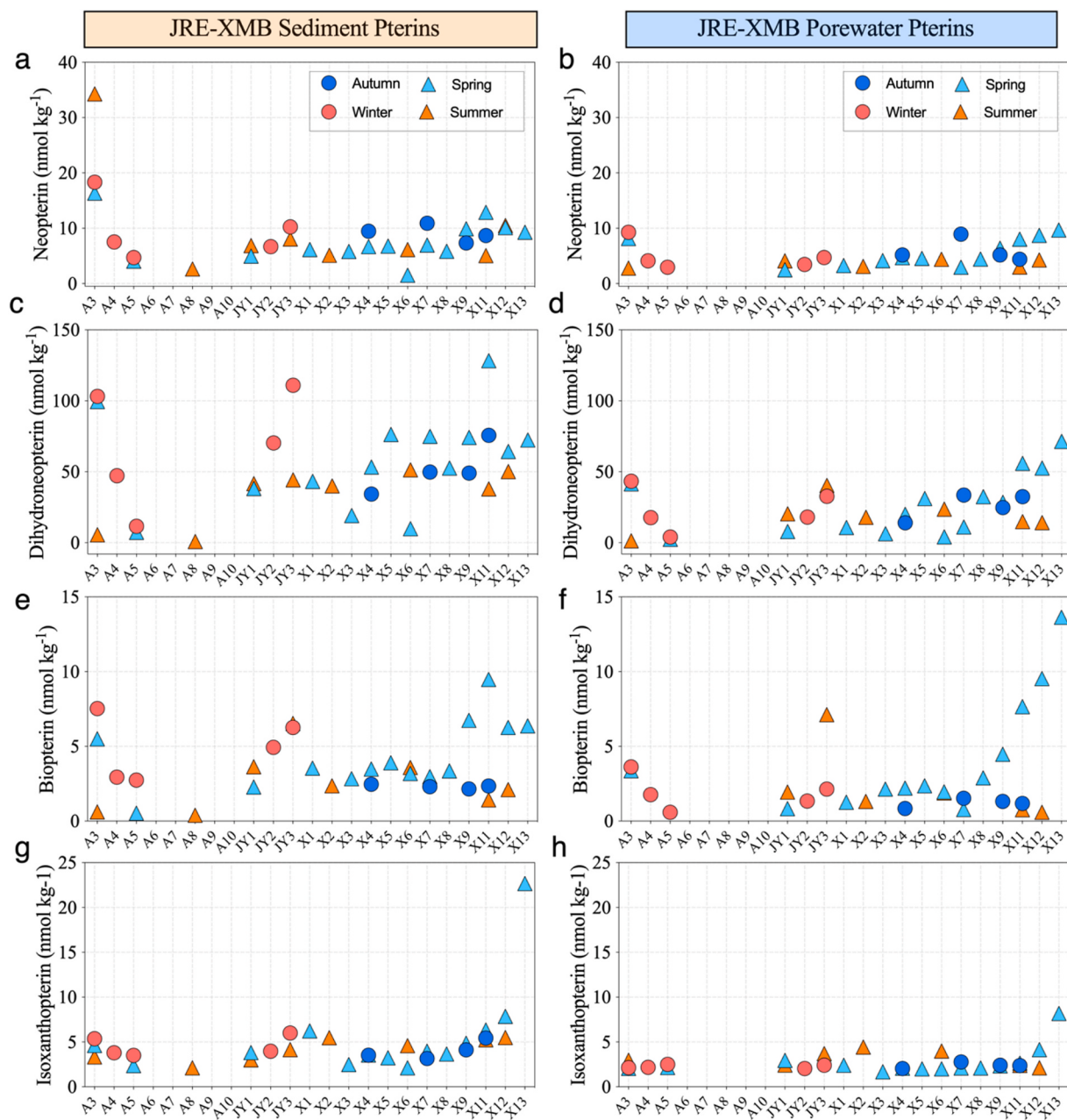


Fig. 1. Seasonal distribution of microbial pterins in surface sediments and their porewater of the Jiulong River Estuary (JRE) and coastal Xiamen Bay (XMB).

(4 mL, v/v 1:1) was added, and the mixture was vortexed for 3 min to extract hydrophilic pterins, with hydrophobic components dissolving into the chloroform. Tubes were centrifuged at 5000 rpm for 10 min, and the aqueous phase was transferred and subjected to a second chloroform extraction (Mashego et al., 2007). Samples were filtered through methanol-rinsed 0.2 µm filters after centrifugation at 5000 rpm for 10 min. Extracts were measured within 48 h or frozen at -20 °C prior to analysis.

High-performance liquid chromatography (HPLC) equipped with a fluorescence detector (FLD, Dionex Ultimate 3000, USA), a quaternary pump (LPG-3400A), an autosampler (WPS-3000SL), a column compartment (TCC-3000), and Chromeleon software was used to record chromatograms and calculate peak areas of pterins. Following a modified method, a Shimadzu-packed VP-ODS column (4.6 × 250 mm, 5 µm) was utilized to separate pterins (Koslinski et al., 2014). The mobile phase consisted of solvent A: chromatographic methanol and solvent B: Milli-Q water in a 10 % A to 90 % B (v/v) ratio. Fluorescent data were

acquired at a flow rate of 0.7 mL min⁻¹ with an injection volume of 20 µL. Excitation and emission spectra were detected using a fluorescence spectrometer at wavelengths of 350 nm and 440 nm, respectively. HPLC-grade methanol and sodium hydroxide were used in all procedures. HPLC-grade hydrochloric acid was obtained from Merck (GR, Germany).

2.4.3. Total pterins calculation

The total pterin ($T_{\text{Pterin}_{\text{sediment}}}$) in both solid and liquid phases was calculated as the sum of solid-phase pterin (S_{Pterin}) and porewater pterin (P_{Pterin}). The total amount of sediment pterins is calculated using Eq. (1):

$$T_{\text{Pterin}_{\text{sediment}}} = S_{\text{Pterin}} + P_{\text{Pterin}} = (M_{\text{solid}} C_{\text{solid}} + V_{\text{liquid}} C_{\text{liquid}}) / M_{\text{solid}} \quad (1)$$

In the formula, $T_{\text{Pterin}_{\text{sediment}}}$ is the total amount of sediment pterins (nmol kg⁻¹) in solid and liquid phases, M_{solid} is the fresh weight of the sediment sample (g), C_{solid} is the content of pterin in solid sediment (nmol kg⁻¹), V_{liquid} is the volume of liquid porewater (mL), C_{liquid} is the

Table 1

Two-way ANOVA of total microbial pterins in the sediments of Jiulong River Estuary (JRE) and coastal Xiamen Bay (XMB) during sampling seasons.

Pterins (nmol kg ⁻¹)	Autumn		Winter		Spring		Summer	
	Aut-XMB	Win-JRE	Spr-JRE	Spr-XMB	Sum-JRE	Sum-XMB		
NP	15.0 ± 3.32b	14.4 ± 7.84B	12.0 ±	11.2 ±	24.9 ± 21.7a	10.4 ±		
DNP	78.5 ± 24.7a	91.8 ± 55.3A	65.6 ±	81.4 ±	38.6 ± 41.2a	62.5 ± 9.59A		
BP	3.52 ± 0.22b	6.77 ± 3.09B	4.17 ±	7.25 ±	5.05 ±	3.5 ± 1.45B		
IP	6.46 ± 0.99b	6.77 ± 1.12B	5.99 ± 1.26a	6.19 ±	5.42 ±	8.44 ±		
				4.27A	2.42a	1.08B		
				1.75B				

Note: Different letters indicate significant differences between pterins in each column ($p < 0.05$); neopterin = NP, dihydro-neopterin = DNP, bioterpin = BP, and isoxanthopterin = IP.

content of pterin in liquid porewater (nmol L⁻¹).

2.5. Microbial composition via genomic analysis

DNA was extracted from the solid phase of suspended particles in water and surface sediments using FastDNA® Spin Kit (MP Biomedical, Santa Anna, CA). The genomic DNA sample was fragmented to 350 bps by sonication. The DNA fragments were then end-polished, A-tailed, and ligated with full-length adapters for Illumina sequencing, followed by PCR amplification. The PCR products were purified using the AMPure XP system (Beverly, USA). Subsequently, library quality was assessed on the Agilent 5400 system (Agilent, USA) and quantified by qPCR. The amplicons were sequenced on Illumina platforms with PE150 by Novogene (Beijing, China). Meanwhile, representative sequences were classified based on operational taxonomic units using the meta micro-database on the Cloud Platform (<https://magic.novogene.com/>).

2.6. Statistical analyses

Differences in pterins among sampling regions were analyzed using two-way ANOVA with Duncan's multiple comparison test. The significance of measured parameters for each pterin was assessed using one-way ANOVA. The Geisser-Greenhouse method corrected variance homogeneity. Mantel tests were performed to assess correlations between pterin distributions (Bray-Curtis dissimilarity) and environmental parameters (Euclidean distance matrices). Significance was set at the level of $p = 0.05$. Spearman analysis identified relationships among parameters. Data statistics and visualizations were conducted using the R statistics package (Version 4.0.2, <https://www.r-project.org>), SPSS Statistics 23.0, and GraphPad Prism 9.

3. Results

3.1. Spatiotemporal variations of pterins in sediments and porewaters

The spatial and seasonal distribution of pterins in estuarine sediments and porewaters revealed distinct redox-driven patterns (Fig. 1). Bioterpin (BP) concentrations were significantly higher ($p < 0.05$) in the outer estuary (JY1–JY3: 7.2–9.0 nmol kg⁻¹), attributed to tidal sediment accumulation, whereas neopterin (NP: 10.4–24.8 nmol kg⁻¹) dominated in the upper estuary under lower salinity regimes (Fig. 1). Conversely, dihydro-neopterin (DNP: 38.6–91.8 nmol kg⁻¹) and bioterpin in the upper estuary decreased during summer, likely due to riverine runoff and erosion in the wet season. Seasonal fluctuations in NP were statistically insignificant ($p > 0.05$), with spatial and redox gradients exerting

Table 2

The ratio of neopterin (NP) and dihydro-neopterin (DNP) in the sediments and the waterbody of the Jiulong River Estuary (JRE) and the coastal Xiamen Bay (XMB).

	Sediment	NP: DNP	Waterbody	NP: DNP	
Autumn	Aut-XMB	0.19	Summer	Surface	1.46
Winter	Win-JRE	0.15			
Spring	Spr-JRE	0.18	Summer	Bottom	1.67
	Spr-XMB	0.14	Autumn	Surface	1.33
Summer	Sum-JRE	0.65			
	Sum-XMB	0.16	Autumn	Bottom	1.19
Ratio (R)		$0 < R < 1$			$1 < R < 2$

stronger control over pterin dynamics (Table 1 and Table 2). Notably, bioterpin exhibited observable but non-significant seasonal trends, peaking in spring/summer (7.2–9.0 nmol kg⁻¹) compared to autumn/winter (5.4–6.8 nmol kg⁻¹). During dry autumn periods, transient increases in bioterpin and isoxanthopterin (IP: 3.5–9.2 nmol kg⁻¹) coincided with reduced hydrological flushing and localized microbial activity.

3.2. Physicochemical characteristics of sediments

Surface sediments primarily consisted of clay (51–93 %), with sand content (4–8 %) increasing near the upper estuary. Coastal sediments in Xiamen Bay had higher clay content (≥ 80 %), while silt content increased in the estuary-bay turbidity zone during the flood seasons (Fig. 2a). Sediment salinity was lower in the estuary due to freshwater inflow from rivers.

Seasonal trends in total organic matter (TOM) and Chl-a concentrations are presented in Fig. 2. The content of TOC (22.1–49.4 g kg⁻¹) correlated positively with Chl-a (0.63–3.84 mg kg⁻¹). Sites in the upper estuary (A3–A5) exhibited higher Chl-a (1.9–3.8 mg kg⁻¹) and TOM, indicating significant input of terrigenous particle organic carbon from freshwater algae.

3.3. Microbial community structure and diversity

The microbial community in estuarine sediments exhibited higher operational taxonomic unit (OUT) diversity than offshore microbial samples, with 34,937 shared OTUs accounting for 12.6 % of the total 277,496 OTUs (Fig. 3a). The microbial community was dominated by taxa adapted to anoxic environments (Fig. 3b), including Gammaproteobacteria, Deltaproteobacteria, Betaproteobacteria (24–48 %), and Anaerolineae (1.7–12 %). These groups are well-documented to thrive under reducing conditions, aligning with the inherent redox stratification of coastal sediments where suboxic/anoxic layers prevail below the surface. Microbial community composition varied spatially: suspended particles were dominated by *Synechococcus* sp. HK05 and uncultured Caudovirales Phage, while sediments featured Anaerolineae and Chloroflexota bacterium at site A8, and Gammaproteobacteria, Chromatiales, and Deltaproteobacteria bacterium at JY1 (Fig. 3c).

3.4. Sediment pterins and chlorophyll-a

Total sediment pterin concentrations exhibited significant positive correlations with Chl-a ($p < 0.001$, $R^2 = 0.26$ –0.46), except for isoxanthopterin (IP; Fig. 4). Bioterpin levels co-varied with Chl-a ($p < 0.05$), aligning with its documented association with photosynthetic cyanobacteria (Lee et al., 1999). In contrast, isoxanthopterin showed no significant linkage to Chl-a ($p = 0.12$), suggesting alternative origins such as heterotrophic metabolism or photodegradation of precursor molecules.

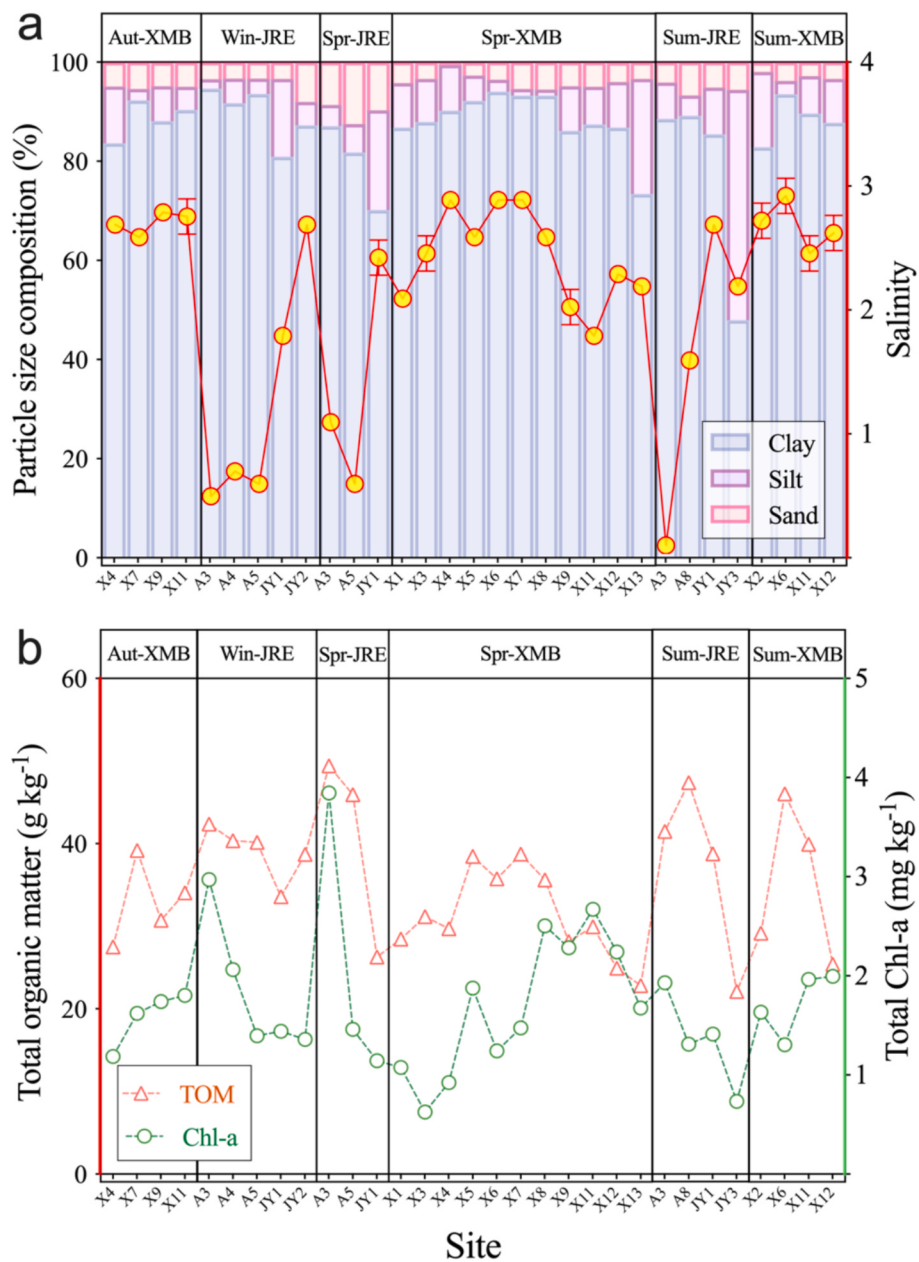


Fig. 2. Distributions of sediment biogeochemical characteristics in the Jiulong River Estuary (JRE) and coastal Xiamen Bay (XMB). (a) Sediment particle constituents and salinity, (b) total organic matter (TOM) and chlorophyll *a* (Chl-*a*) in the sediments.

3.5. Pterin associations with organic carbon pools

Total organic carbon (TOC: 0.57–1.31 %) and total nitrogen (TN: 0.18–0.36 %) displayed strong correlations ($R^2 > 0.9$) in both Jiulong River Estuary (JRE) and XMB (Fig. 6). TOC and TN peaked in the upper estuary (A3–A5) and declined downstream (JY1–JY3), with seasonal maxima in autumn and winter (Fig. 2).

The isoxanthopterin content was positively correlated with the C/N ratio in JRE (C/N: 8.21–10.26) and XMB (C/N: 8.90–10.5), as shown in Fig. 5. During flood periods, isoxanthopterin concentrations and C/N ratios decreased from the upper estuary to the sea in JRE. In XMB, higher isoxanthopterin concentrations in the inner bay (X7–X13) corresponded to lower C/N ratios (Fig. 1). There was a significant positive correlation between isoxanthopterin and C/N ($R^2 = 0.65$, $p < 0.001$, Fig. 5b). In the coastal waters of XMB, lower isoxanthopterin concentrations were found near the estuary, while higher concentrations in the inner Bay (X7–X13) corresponded to lower C/N ratios. The C/N ratio decreased with

increasing isoxanthopterin content (Fig. 5c).

Mantel tests identified pH ($p < 0.01$) and C/N ($p < 0.05$) as key drivers of sediment pterin variability in JRE, while porewater pterins correlated with TN ($p < 0.05$; Fig. 6a). In XMB, sediment and porewater pterins were strongly linked to Chl-*a*, clay content, and salinity ($p < 0.01$; Fig. 6b). In contrast, XMB sediments showed strong correlations between total sediment and porewater pterins with sediment Chl-*a*, total Chl-*a*, clay content, and salinity ($p < 0.01$).

4. Discussion

4.1. Spatiotemporal dynamics of pterins in response to environmental drivers

Our findings demonstrate that the concentrations of pterins in sediments across all seasons followed the order of DNP > NP > BP > IP (Fig. S3). Dihydro-neopterin (44–60.8 nmol kg⁻¹) in sediments was an

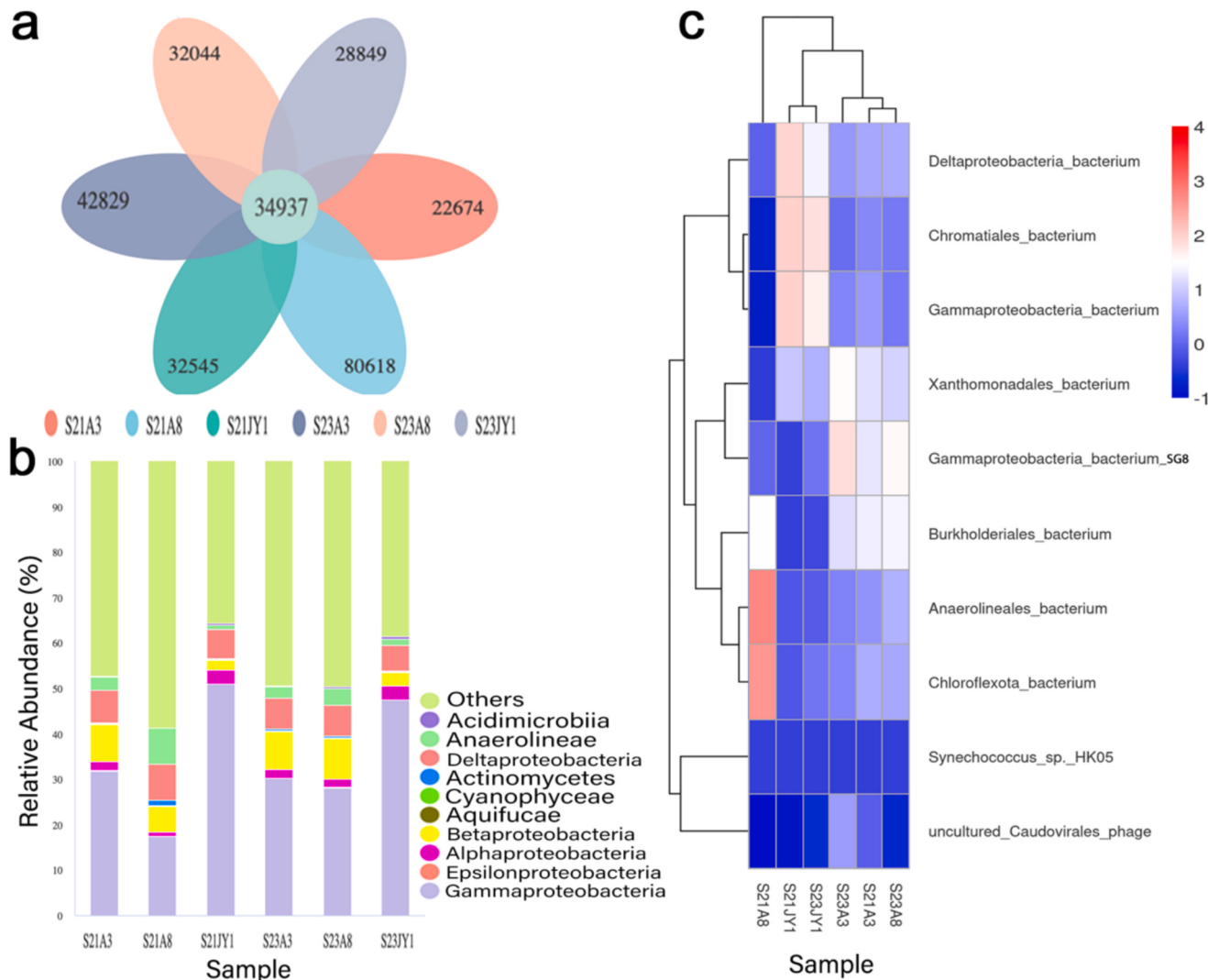


Fig. 3. Relative abundance and cluster analysis of bacterial community at different genus levels of the collected sediments. (a) Venn diagram of gene numbers in surface sediments, (b) Relative abundance of the abundant species; (c) Species results of bacterial community in the surface sediments.

order of magnitude higher than biopterin ($5.0\text{--}9.5\text{ nmol kg}^{-1}$). During spring, both dihydro-neopterin and biopterin concentrations were elevated in high-salinity sites (X9–X13, Fig. 1). Lower sediment salinity in the estuary, driven by freshwater influx from river discharge, likely contributes to this pattern (Yu et al., 2019).

Historical data indicate that harmful algae blooms (HABs) frequently occur in Tong'an Bay (X8–X12) during spring and summer, accounting for up to 40.5 % of regional red tides over the past three decades (Chen et al., 2021). The increased biopterin levels observed during this period may be linked to algal growth and proliferation, evident in both sediment and water samples. Biopterin concentrations in porewater and sediments were consistently distributed across seasons, with higher levels observed at the estuarine upstream and downstream boundaries. Notably, average biopterin levels in sediments were higher than those in porewater (Fig. S2). In spring, porewater biopterin concentrations gradually increased from the inner bay to the outer channel (X7–X13, Fig. 1), which can be attributed to elevated productivity (Chen et al., 2021).

Mantel test analysis revealed significant correlations between pterins in sediments and environmental factors such as pH ($p < 0.01$) and the C/N ratio ($p < 0.05$, Fig. 6a). In contrast, biopterin levels in porewater were primarily correlated with TN content ($p < 0.05$). Sediment pH strongly influences microbial activity, which in turn affects biopterin levels.

Previous studies highlight that sediment pH and redox conditions regulate microbial populations and hydrocarbon mineralization rates, with peak activity at pH 8.0 and reduced rates at pH 5.0 (Hambrick et al., 1980). Variations in the C/N ratio and biopterin distribution suggest microbial pterins act as biomarkers, indicative of significant exogenous microbial contributions in estuarine sediments.

Porewater pterin concentrations in XMB were significantly correlated with sediment pterins and Chl-a ($p < 0.01$, Fig. 6b), as well as clay content and salinity ($p < 0.01$). These correlations suggest that sedimentary Chl-a and porewater pterins may share common sources. Elevated clay content likely enhances porewater retention and sediment salinity, fostering microbial activity. Overall, sediment pH and C/N ratios in coastal waters and particle size composition, sediment Chl-a and porewater salinity in coastal waters emerged as key factors driving the spatiotemporal distribution of microbial pterins.

4.2. Relationship between sediment pterin and chlorophyll a

A significant positive correlation was observed between sediment pterin and sediment Chl-a, with the exception of isoxanthopterin (Fig. 4). Elevated Chl-a content corresponded to higher pterin levels, underscoring autotrophic organisms as a primary source of microbial pterins. Biopterin's association with phytoplankton biomass reflects its

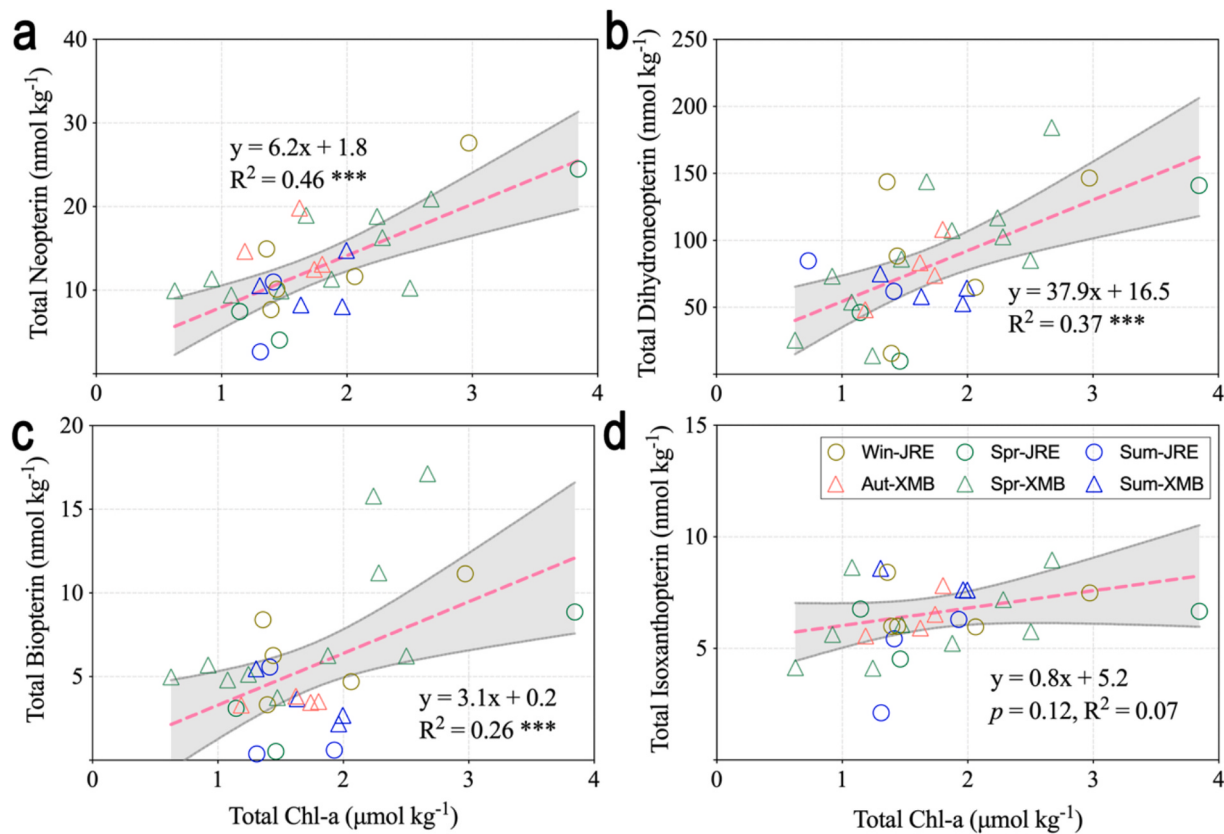


Fig. 4. The linear correlation of sediment total microbial pterins and chlorophyll of four seasons in the Jilong River Estuary (JRE) and coastal Xiamen Bay (XMB). The symbol (***) represents a significant difference at the significance of $p < 0.001$. The grey line is the 95 % confidence interval.

abundance in cyanobacteria, where pterin glycosides participate in photosynthetic electron transport (Forrest et al., 1957; Hatfield et al., 1961; Lee et al., 1999).

The significant correlation ($R^2 = 0.98$) between cyanopterin and Chl-a during *Synechocystis* sp. PCC 6803 cultivation, with a molar ratio of ~1:1.6, highlights cyanobacteria as a major contributor to biopterin production (Lee et al., 1999). The uncoupled correlation between isoxanthopterin and Chl-a ($p = 0.12$, Fig. 4d) suggests isoxanthopterin originates primarily from diverse sources, where its functions as bacterial pigments (Coble, 1989) or a carbon source for microbes (McNutt, 1963). Additionally, biopterin glucoside in cyanobacteria can degrade into isoxanthopterin through photodegradation and oxidation (Lee et al., 1999), providing an alternative source.

4.3. Pterins as potential biomarkers for organic carbon dynamics

C/N ratios in JRE (8.21–10.26) and XMB (8.90–10.5) sediments showed a linear correlation with isoxanthopterin contents (Fig. 5b, c). The C/N ratio, combined with $\delta^{13}\text{C}$, reflects organic matter sources, such as marine algae, terrestrial inputs, and freshwater algae (Lamb et al., 2006). Higher C/N values indicate terrestrial organic carbon inputs, while lower C/N values suggest faster nitrogen mineralization and bacterial utilization by (Hodge et al., 2000).

In flood seasons, JRE transports large amounts of terrestrial organic carbon and freshwater algae, leading to decreasing isoxanthopterin content and C/N ratios downstream. This reflects dilution and sedimentation of terrestrial organic matter (Lamb et al., 2006; Wang and Wang, 2017; Yu et al., 2019). In XMB, the stable C/N ratio and increased isoxanthopterin levels suggest that marine algae and bacteria as primary contributors, distinct from terrestrial influences. Isoxanthopterin's association with C/N ratios may reflect microbial processing of labile organic matter, indirectly informing carbon degradability. However, its

utility as a direct proxy for net carbon burial requires validation through sediment flux measurements and isotopic tracers. This preliminary evidence underscores the need to integrate pterin dynamics into broader carbon sequestration models.

Isoxanthopterin production in sediments is influenced by heterotrophic bacteria and environmental conditions such as light and oxygen. Biopterin and isoxanthopterin are particularly sensitive to degradation, transforming into derivatives such as pterin-6-carboxylic acid under photic and oxidative conditions (Jung-Klawitter and Kuseyri Hübschmann, 2019). Reduced sediment conditions promote neopterin and dihydro-neopterin biosynthesis, while biopterin and isoxanthopterin concentrations remain low due to degradation or consumption.

5. Implications and limitations

Pterin distributions reflect niche-specific microbial activity, with biopterin and dihydro-neopterin serving as complementary indicators of algal blooms and redox states, respectively. The variation in pterin species (e.g., dihydro-neopterin in sediments, biopterin in water) reflects redox states and microbial activity in coastal environments. The neopterin-to-dihydro-neopterin ratio differed between sediments (0.14–0.65, NP < DNP) and waterbodies (1.19–1.67, NP > DNP), highlighting redox-dependent dynamics (Table 2). Neopterin and biopterin serve as cofactors in redox reactions and protect against oxidative stress (Basu and Burgmayer, 2011a; Feirer and Fuqua, 2017).

Minimal seasonal variation in sedimentary dihydro-neopterin contrasts with biopterin's responsiveness to nutrient inputs, highlighting differential controls on pterin production. Biopterin, dihydro-neopterin, and isoxanthopterin concentrations positively correlated with nutrients and Chl-a, suggesting their utility as complementary biomarkers for monitoring algal blooms. Seasonal dynamics indicate nutrient input and freshwater organic carbon during flood seasons drive microbial pterin

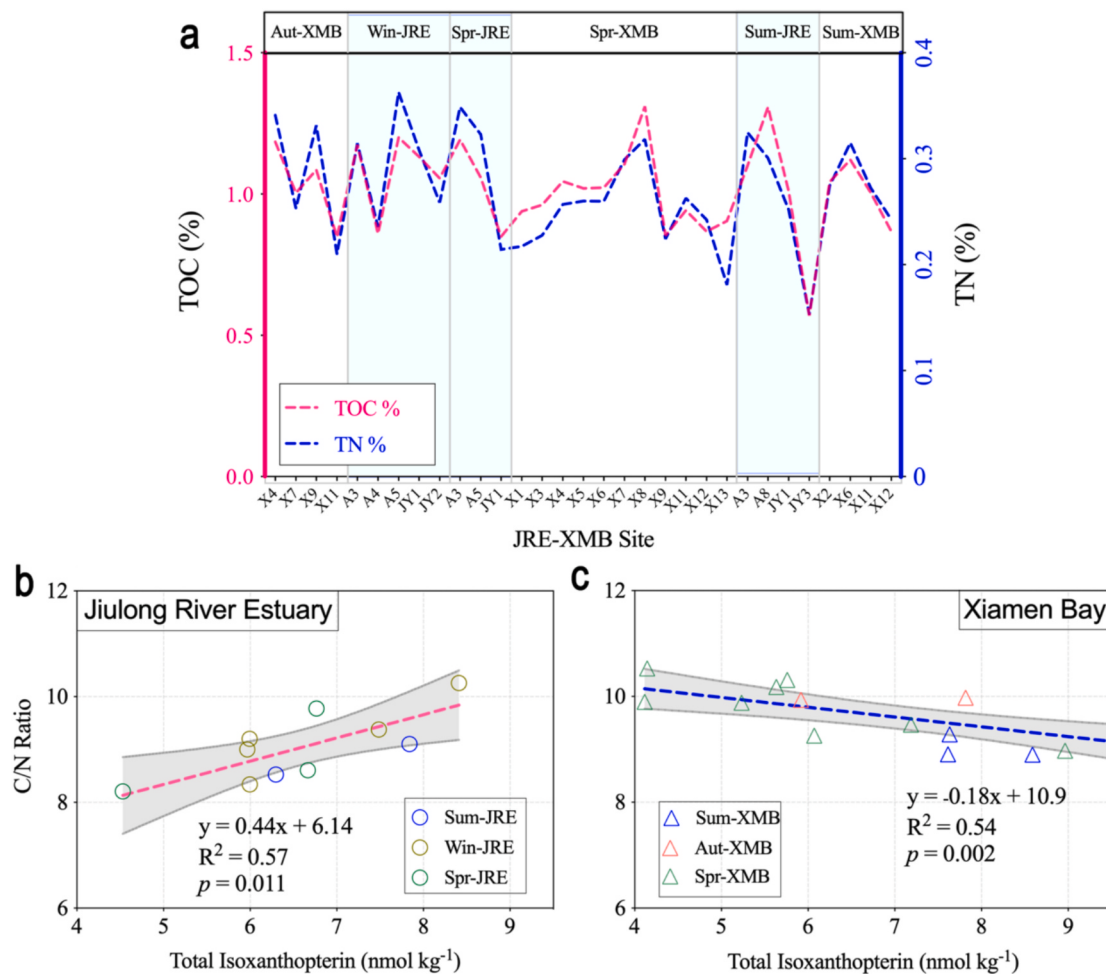


Fig. 5. The linear correlation of sediment microbial pterins and chlorophyll of four seasons in the Jiulong River Estuary (JRE, light-cyan bar) and Xiamen Bay (XMB). (a) Total organic carbon and total nitrogen of four seasons in the Jiulong River Estuary (JRE, light-cyan bar) and Xiamen Bay (XMB). The grey line is the 95 % confidence interval. (For interpretation of the references to colour in this figure legend, the reader is referred to the web version of this article.)

production, with photoautotrophic microorganisms dominating in high-productivity zones and heterotrophs prevailing in reduced environments. The accumulation and consumption of pterins by microorganisms indicate that measured microbial pterins reflect intracellular dynamic levels rather than the actual flux of microbial synthesis and utilization. Future research should focus on linking specific pterin species to microbial phenotypes, their roles in carbon metabolism, and interactions with environmental factors.

6. Conclusions

Our findings reveal that microbial pterins exhibit distinct spatio-temporal patterns in estuarine sediments, closely linked to seasonal hydrological shifts and redox conditions. During flood seasons, phytoplankton-derived pterins dominate, driven by high primary productivity from upstream inputs, while heterotrophic contributions prevail in dry seasons and reducing sediments. The strong correlation between chlorophyll-a (Chl-a) and pterin levels highlights their co-variation with algal biomass, suggesting their potential as complementary indicators for monitoring bloom dynamics. Similarly, the association of isoxanthopterin with sediment C/N ratios points to its role in reflecting organic carbon degradability, though this relationship requires further mechanistic validation. While pterin and Chl-a correlations align with autotrophic activity, these relationships likely reflect shared environmental drivers (e.g., nutrient availability) rather than direct metabolic causality. Future isotope tracing studies are essential to

resolve pterin production pathways. Laboratory experiments with controlled pterin additions are needed to establish causality.

As the first systematic investigation of microbial pterins in subtropical estuarine sediments, this study provides foundational insights into their biogeochemical significance. However, we emphasize that observed correlations do not imply direct causality; rather, they underscore the need for targeted laboratory experiments (e.g., pterin addition/removal studies) and multi-omics approaches to unravel microbial metabolic pathways. Future work should also integrate pterin dynamics into carbon flux models to assess their diagnostic utility in coastal carbon sink evaluation.

In summary, while microbial pterins show promise as biomarkers, their diagnostic utility hinges on resolving metabolic pathways through controlled experiments. This study provides a critical baseline for future hypothesis-driven research and bridges a critical gap in marine biogeochemistry and sets the stage for advancing pterin-based monitoring frameworks in rapidly changing estuarine ecosystems.

Declaration of Generative AI and AI-assisted technologies in the writing process

During the preparation of this work, the author(s) used ChatGpt (OpenAI) to improve the manuscript's linguistic expression and readability. After using this tool/service, the author(s) reviewed and edited the content as needed and take(s) full responsibility for the content of the publication.

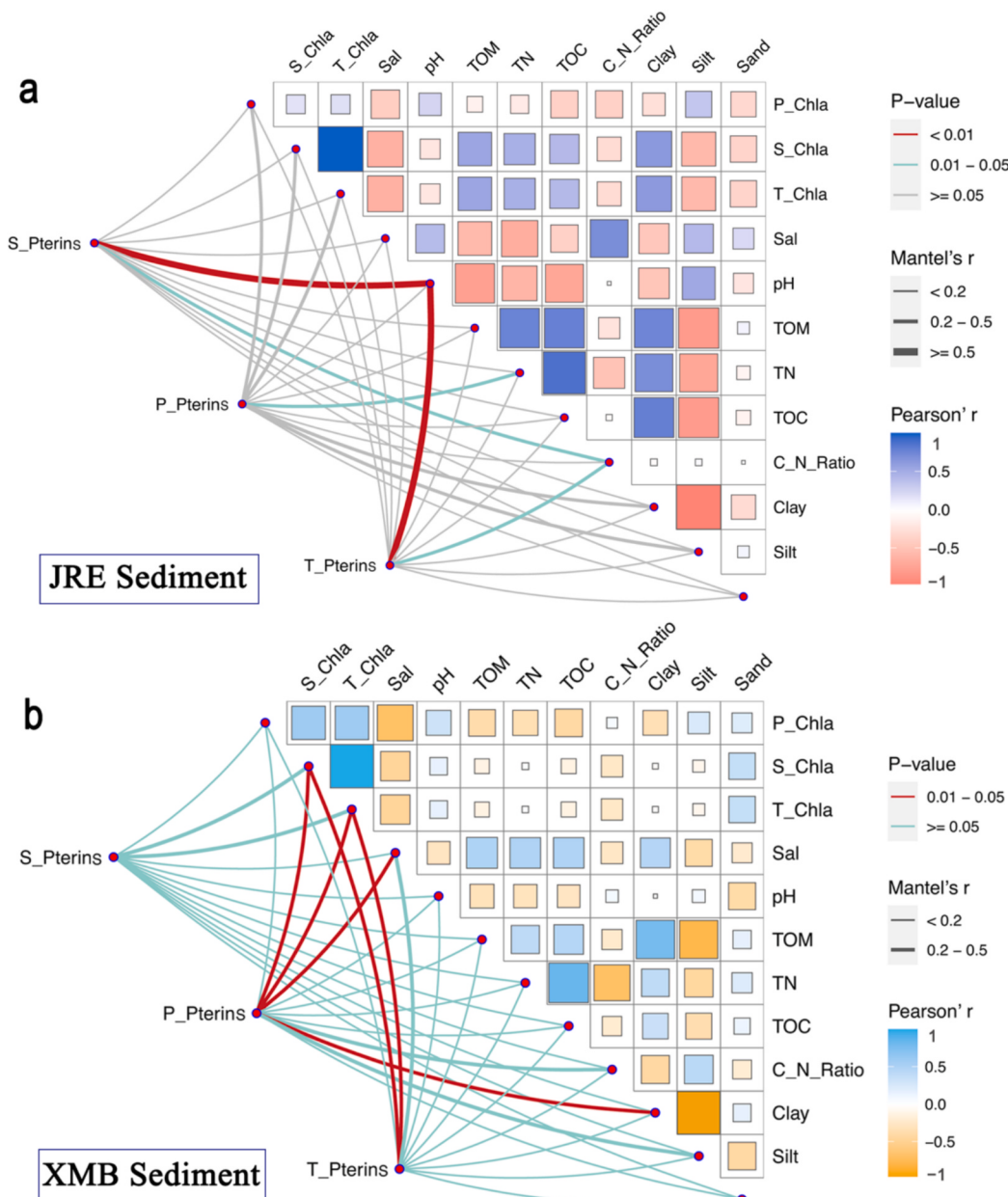


Fig. 6. Mantel analysis of microbial pterins in response to environmental factors in surface sediments in the Jilong River Estuary (JRE) and coastal Xiamen Bay (XMB). (a) Surface sediments in the JRE, (b) Surface sediments in the XMB; Sediment Pterins = S_Pterins, Porewater Pterins = P_Pterins, Total Pterins = T_Pterins.

CRediT authorship contribution statement

Kang Mei: Writing – review & editing, Writing – original draft, Software, Methodology, Investigation, Formal analysis, Data curation, Conceptualization. **Yitong Pan:** Writing – original draft, Visualization. **Danny Alejandro Osorio:** Writing – original draft. **Lizhe Cai:** Supervision, Resources, Project administration, Funding acquisition. **Hualong Hong:** Resources, Methodology, Conceptualization. **Mohammad Mazzbah Uddin:** Writing – original draft. **Song Wang:** Writing – review & editing, Formal analysis. **Xin Xiao:** Writing – review & editing, Formal analysis. **Xuri Dong:** Writing – review & editing, Formal analysis. **Li Chen:** Writing – review & editing, Formal analysis. **Shicong Xiao:** Writing – review & editing, Formal analysis. **Deli Wang:** Supervision, Resources, Project administration, Funding acquisition.

Declaration of competing interest

The authors declare that they have no known competing financial interests or personal relationships that could have appeared to influence the work reported in this paper.

Acknowledgment

This study was supported by the Start-up Funding for Young Researchers (at Jiangsu Ocean University and the Youth Funding of the Jiangsu Natural Science Foundation (BK20241063). Partial funding was provided by the National Natural Science Foundation of China (NSFC) under grants 41476060 and U1805242. We sincerely thank Liuqian Qi, Haowen Zhong, Xinli Yue, and Wenmei Liu for their valuable assistance with sampling and laboratory analyses. We also extend special gratitude to Professor Sergio A. Sañudo-Wilhelmy from the University of Southern California, USA, for his invaluable guidance and encouragement during

my stay in his laboratory, which has greatly inspired further research on pterins in marine sciences.

Appendix A. Supplementary material

Supplementary data to this article can be found online at <https://doi.org/10.1016/j.catena.2025.109147>.

References

- Arpa, E.M., Corral, I., 2023. Unveiling photodegradation and photosensitization mechanisms of unconjugated pterins. *Chem.-Eur. J.*, e202300519.
- Basu, P., Burgmayer, S.J., 2011. Pterin chemistry and its relationship to the molybdenum cofactor. *Coord. Chem. Rev.* 255, 1016–1038.
- Batchelli, S., Muller, F.L., Chang, K.C., Lee, C.L., 2010. Evidence for strong but dynamic iron-humic colloidal associations in humic-rich coastal waters. *Environ. Sci. Technol.* 44, 8485–8490.
- Bruland, K.W., Lohan, M.C., 2004. The control of trace metals in seawater. *Oceans Mar. Geochem.*
- Bufflap, S.E., Allen, H.E., 1995. Sediment pore water collection methods for trace metal analysis: a review. *Water Res.* 29, 165–177.
- Buglak, A.A., Kapitonova, M.A., Vechtomova, Y.L., Telegina, T.A., 2022. Insights into molecular structure of pterins suitable for biomedical applications. *Int. J. Mol. Sci.* 23, 15222.
- Cai, W.-J., et al., 2021. Natural and anthropogenic drivers of acidification in large estuaries. *Ann. Rev. Mar. Sci.* 13, 23–55.
- Chen, B.H., Kang, W., Xu, D., Hui, L., 2021. Long-term changes in red tide outbreaks in Xiamen Bay in China from 1986 to 2017. *Estuarine Coast. Shelf Sci.* 249.
- Chung, H.J., et al., 2000. Purification and characterization of UDP-glucose: tetrahydrobiopterin glucosyltransferase from *Synechococcus* sp. PCC 7942. *BBA* 1524, 183–188.
- Coble, P.G., 1989. Marine Bacteria as a Source of Dissolved Fluorescence in the Ocean. Massachusetts Institute of Technology.
- Daubner, S.C., Fitzpatrick, P.F., 2013. Pteridines. *Encyclopedia of Biol. Chem.* 12, 666–669.
- Feirer, N., Fuqua, C., 2017. Pterin function in bacteria. *Pteridines* 28, 23–36.
- Forrest, H.S., Van Baalen, C., Myers, J., 1957. of Pteridines in a blue-green alga. *Science* 125, 699–700.
- Forrest, H.S., Van Baalen, C., Myers, J., 1958. Isolation and identification of a new pteridine from a blue-green alga. *Arch. Biochem. Biophys.* 78, 95–99.
- Gorelova, V., et al., 2019. Evolution of folate biosynthesis and metabolism across algae and land plant lineages. *Scientific Reports* 9, 5731.
- Guo, W.D., 2005. Fluorescent characteristics of colored dissolved organic matter (CDOM) in the Jiulong River Estuary. *Oceanologia Et Limnologia Sinica* 36, 349–357.
- Hambrick III, G.A., Delaune, R.D., Patrick Jr., W., 1980. Effect of estuarine sediment pH and oxidation-reduction potential on microbial hydrocarbon degradation. *Appl. Environ. Microbiol.* 40, 365–369.
- Han, 2019. Source identification and water-quality assessment of dissolved heavy metals in the Jiulongjiang River, Southeast China. *J. Coast. Res.* 36.
- Hatfield, D., Van Baalen, C., Forrest, H., 1961. Pteridines in blue green algae. *Plant Physiol.* 36, 240.
- Hodge, A., Stewart, J., Robinson, D., Griffiths, B., Fitter, A., 2000. Competition between roots and soil micro-organisms for nutrients from nitrogen-rich patches of varying complexity. *J. Ecol.* 88, 150–164.
- Jung-Klawitter, S., Kuseyri Hübschmann, O., 2019. Analysis of catecholamines and pterins in inborn errors of monoamine neurotransmitter metabolism—from past to future. *Cells* 8, 867.
- Koslinski, P., Jarzemski, P., Markuszewski, M.J., Kalisz, R., 2014. Determination of pterins in urine by HPLC with UV and fluorescent detection using different types of chromatographic stationary phases (HILIC, RP C-8, RP C-18). *J. Pharm. Biomed. Anal.* 91, 37–45.
- Lamb, A.L., Wilson, G.P., Leng, M.J., 2006. A review of coastal palaeoclimate and relative sea-level reconstructions using ^{81}C and C/N ratios in organic material. *Earth Sci. Rev.* 75, 29–57.
- Lee, H.W., Oh, C.H., Geyer, A., Pfeiderer, W., Park, Y.S., 1999. Characterization of a novel unconjugated pteridine glycoside, cyanopterin, in *Synechocystis* sp. PCC 6803. *Bioenergetics* 1410, 61–70.
- Lei, P., Chen, M., Rong, N., Tang, W., Zhang, H., 2023. A passive sampler for synchronously measuring inorganic and organic pollutants in sediment porewater: configuration and field application. *J. Environ. Sci.*
- Liu, N., et al., 2017. Carbon assimilation and losses during an ocean acidification mesocosm experiment, with special reference to algal blooms. *Mar. Environ. Res.* 129, 229–235.
- Lu, W., et al., 2017. Contrasting ecosystem CO₂ fluxes of inland and coastal wetlands: a meta-analysis of eddy covariance data. *Glob. Chang. Biol.* 23, 1180–1198.
- Lu, Z., et al., 2023. Salt marsh invasion reduces recalcitrant organic carbon pool while increases lateral export of dissolved inorganic carbon in a subtropical mangrove wetland. *Geoderma* 437, 116573.
- Mao, S.-H., et al., 2022. Aerobic oxidation of methane significantly reduces global diffuse methane emissions from shallow marine waters. *Nat. Commun.* 13, 7309.
- Mashego, M.R., et al., 2007. Microbial metabolomics: past, present and future methodologies. *Biotechnol. Lett.* 29, 1–16.
- Matsunaga, T., et al., 1993. An Ultraviolet (Uv-a) Absorbing Biopterin Glucoside from the Marine Planktonic Cyanobacterium Oscillatoria Sp. *Appl. Microbiol. Biotechnol.* 39, 250–253.
- McNutt Jr., W.S., 1963. The metabolism of isoxanthopterin by *Alcaligenes faecalis*. *J. Biol. Chem.* 238, 1116–1121.
- Mei, K., et al., 2020. The migrated behavior and bioavailability of arsenic in mangrove sediments affected by pH and organic acids. *Mar. Pollut. Bull.* 159, 111480.
- Mei, K., et al., 2023. Stimulation of oxalate root exudate in arsenic speciation and fluctuation with phosphate and iron in anoxic mangrove sediment. *Mar. Pollut. Bull.* 189, 114823.
- Pan, F., et al., 2021. Kinetic characteristics of mobile Mo associated with Mn, Fe and S redox geochemistry in estuarine sediments. *J. Hazard. Mater.* 418, 126200.
- Suffridge, C., Cutter, L., Sanudo-Wilhelmy, S.A., 2017. A New Analytical Method for Direct Measurement of Particulate and Dissolved B-vitamins and Their Congeners in Seawater. In: *Frontiers in Marine Science*, p. 4.
- Wachi, Y., et al., 1995. Effect of Ultraviolet-a (Uv-a) Light on Growth, Photosynthetic Activity and Production of Biopterin Glucoside by the Marine Uv-a Resistant Cyanobacterium Oscillatoria Sp. *BBA-Gen. Subjects* 1244, 165–168.
- Wang, W., Wang, W.-X., 2017. Trace metal behavior in sediments of Jiulong River Estuary and implication for benthic exchange fluxes. *Environ. Pollut.* 225, 598–609.
- Wang, W.H., Chen, M., Guo, L.D., Wang, W.X., 2017. Size partitioning and mixing behavior of trace metals and dissolved organic matter in a South China estuary. *Sci. Total Environ.* 603, 434–444.
- Wang, W.H., Wang, W.X., 2016. Phase partitioning of trace metals in a contaminated estuary influenced by industrial effluent discharge. *Environ. Pollut.* 214, 35–44.
- Xie, M., et al., 2023. The high organic carbon accumulation in estuarine wetlands necessarily does not represent a high CO₂ sequestration capacity. *Environ. Int.* 172, 107762.
- Yu, D., et al., 2019. Understanding how estuarine hydrology controls ammonium and other inorganic nitrogen concentrations and fluxes through the subtropical Jiulong River Estuary, SE China under baseflow and flood-affected conditions. *Biogeochemistry* 142, 443–466.
- Zuo, Y.-T., et al., 2022. Identification of pterins as characteristic humic-like fluorophores released from cyanobacteria and their behavior and fate in natural and engineered water systems. *Chem. Eng. J.* 428, 131154.